Journal of the Serbian Chemical Society
JSCS-info@shd.org.rs • www.shd.org.rs/JSCS
J. Serb. Chem. Soc. *87* (4) 465–477 (2022)
JSCS–5534
Original scientific paper
Published 8 March 2022

Investigations on the role of cation–π interactions in active centres of superoxide dismutase

SRĐAN Đ. STOJANOVIĆ[1] and MARIO V. ZLATOVIĆ[2]*#

[1]*University of Belgrade-Institute of Chemistry, Technology and Metallurgy, Department of Chemistry, Belgrade, Serbia and* [2]*Faculty of Chemistry, University of Belgrade, Belgrade, Serbia*

(Received 9 January, revised 17 February, accepted 21 February 2022)

Abstract: In this study, we have analysed the influence of cation–π interactions on stability and properties of superoxide dismutase (SOD) active centres. The number of interactions formed by arginine is higher than by lysine in the cationic group, while those formed by histidine are comparatively higher in the π group. The energy contribution resulting from most frequent cation–π interactions was in the lower range of strong hydrogen bonds. The cation–π interactions involving transition metal ions as cation have energy more negative than –418.4 kJ mol^{-1}. The stabilization centres for these proteins showed that all the residues involved in cation–π interactions were important in locating one or more of such centres. The majority of the residues involved in cation–π interactions were evolutionarily conserved and might have a significant contribution towards the stability of SOD proteins. The results presented in this work can be very useful for understanding the contribution of cation–π interactions to the stability of SOD active centres.

Keywords: superoxide dismutase; cation–π interactions; catalytic site.

INTRODUCTION

Non-covalent interactions maintain an intricate balance between the rigidity and the flexibility in proteins. Understanding the balance of non-covalent interactions is vital for the stability and interactivity of biological macromolecules.[1] Cation–π interactions, as an ensemble of noncovalent attraction, play an important role in many areas ranging from molecular biology to materials design.[2–7] In biology, consenting cations can be found in the basic side chains of proteins, as well as in many different ligands, toxins, other small molecules, or even ions that might closely interact with the protein. Similarly, the π-electron partner in a

* Corresponding author. E-mail: mario@chem.bg.ac.rs
# Serbian Chemical Society member.
https://doi.org/10.2298/JSC220109013S

cation–π interaction can be provided either by aromatic side chains (Phe, Tyr or Trp), or by an aromatic moiety of an interacting ligand. Note that the side chain of histidine may formally act as a cation or as an aromatic group, thus requiring particular consideration.[8] For the guanidinium moiety of arginine (a dispersed π-system itself) the side chain can interact with an aromatic through parallel (stacking) or perpendicular (T-shaped) geometries.[9]

The cation–π interaction is electrostatic in its nature, because the major contributions arise from the electrostatic attractions between cations and the quadrupole moment of the aromatics.[10] This type of noncovalent interaction can be very strong, as has been showed by the solid-state studies of small-molecule crystal structures.[11,12] and by theoretical and experimental analyses in the gas phase and in aqueous media.[12–14] The strength of cation–π interactions ranges between 8.4 and 627.6 kJ mol^{-1},[15] sometimes comparable to the strong hydrogen bonds. Its strength critically depends on the nature of aromatic system and charge of the cation.[2] Depending on the type of cations and the nature of the π system, it can be regulated to be weak as well. The adjustability of cation–π interaction offers a potential strategy modification of the neighbouring environment, where it is involved. Cation–π interactions are therefore considered to be an essential force in generating tertiary and quaternary protein structures induced by oligomerization and protein folding.[16]

Hence, we attempted to explore the nature, range, strength, and significance of the cation–π interactions in SOD proteins, which could help in understanding the protein stability and mechanism, and similarly in protein-engineering and modelling.

EXPERIMENTAL

Dataset

For this study, we used the Protein Data Bank (PDB), accessed on May 10th, 2021, at that moment listing 183,118 resolved structures.[17] The selection criteria for superoxide dismutase to be included in the dataset were as follows: 1) crystal structures of proteins containing E.C. Number 1.15.1.1 (superoxide dismutase) with metal were accepted; 2) theoretical model structures and NMR structures were not included (these structures were not accepted as it was difficult to define the accuracy of the ensemble of structures in terms of displacement that was directly comparable to the X-ray diffraction studies); 3) only crystal structures with the resolution of 0.2 nm or better and a crystallographic *R*-factor of 25.0 % or lower were accepted; 4) we included only representatives having at least 30 % sequence identity. After assembling the dataset, several structures containing ligands and mutant amino acids were rejected, leaving 43 proteins that were actually used as the dataset in our analysis. Hydrogen atoms were added and optimized, where needed, using the program REDUCE,[18] with default settings. REDUCE software adds hydrogen atoms to protein and/or DNA structures in standardized geometry, optimizing them to the orientations of OH, SH, NH_3^+, Met methyls, Asn and Gln sidechain amides, and His rings. The applied software determines the best hydrogen positions by selecting the best overall score from all the possible combinations, taking into the account single scores assigned for each individual residue and for groups containing movable

protons partitioned in closed sets of local interacting networks. The PDB IDs of selected structures were as follows: 1ar5, 1cbj, 1d5n, 1hl5, 1ids, 1isa, 1kkc, 1luv, 1my6, 1qnn, 1srd, 1to4, 1unf, 1xre, 1xuq, 1y67, 1yai, 1yso, 2aqn, 2cw2, 2goj, 2rcv, 2w7w, 3ak2, 3ce1, 3dc6, 3evk, 3f7l, 3h1s, 3js4, 3lio, 3lsu, 3mds, 3pu7, 3tqj, 4br6, 4c7u, 4f2n, 4ffk, 4yet, 5a9g, 5vf9 and 6bej.

Cation–π interaction analysis

For selecting the protein structures having various types of cation–π interactions, Discovery Studio Visualizer 2020 was used,[19] with some specific criteria and geometrical feature settings. The following tests were performed to find cation–π interactions: 1) cations were considered to be an atoms having a formal charge of at least +0.5 to allow the inclusion of delocalized cationic species such as lysine and arginine side chains; 2) the distance (*R*) between a cation and the centroid of a π ring should be less than the π–cation (max dist) cutoff (0.7 nm by default, see *R* in Fig. 1); 3) The angle (θ) between the cation–centroid vector and the normal to the ring plane should be less than the π–cation maximum angle (45° by default, see θ in Fig. 1). The aromatic systems include the aromatic side chains of the residues tryptophan (Trp), tyrosine (Tyr), phenylalanine (Phe), and histidine (His). All the metal ions present in the database are treated as cations, apart from the protonated basic amino acid residues lysine (Lys) and arginine (Arg). However, as His can act either as cation or as an aromatic moiety depending on its protonation state, in our study both the possibilities are considered.

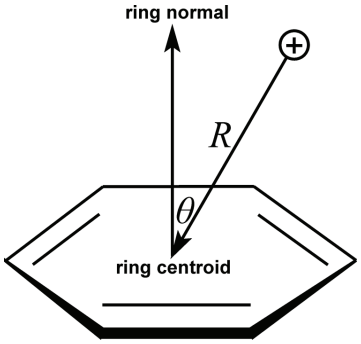

Fig. 1. Parameters for cation–π interactions: (*R*) the distance between the cation and the centroid; (θ) the angle between the cation-centroid vector and the normal to the ring plane. The figure was derived from parameters described in this subsection.

Computation of cation–π interaction energy

In order to apply *ab initio* methods in determining the energies of cation–π pairs on desired level of theory, with sufficient level of accuracy and still in satisfactory time frame, calculations were performed on structurally reduced model systems.[20] We used butan-1-amine (**1**) and 2-propylguanidine (**2**) as mimics for lysine and arginine groups, respectively. Phenylalanine was simplified to toluene (**3**), histidine to 5-methyl-1*H*-imidazole (**4**), tryptophan to 3-methyl-*H*-indole (**5**) and tyrosine was reduced to 4-methylphenol (**6**), Fig. 2.

The use of reduced model systems in calculations of specific intramolecular interaction in large systems is a well known and already proved methodology,[21] producing accurate enough results, and still significantly reducing computation times and strength needed for them. Larger models, like whole amino acids, or parts of protein chain, will unnecessary complicate calculations and probably even bring in errors. Numerous interactions mechanisms are possible in a larger protein structure, and a single binding energy computation cannot always correctly determine which of these interactions are present and to what amount they contribute to overall stabilization. As a result, separating the involvement of the cation–π interaction and

their energy contributions from the interacting pair residues involved in other noncovalent interactions is difficult.

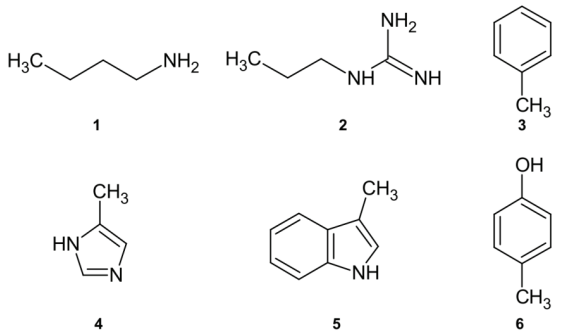

Fig. 2. Structurally reduced structures used for calculations of cation–π interaction energy. (**1**) instead of lysine; (**2**) instead of arginine; (**3**) instead of Phe; (**4**) instead of His; (**5**) instead of Trp; (**6**) instead of Tyr.

Ab initio calculations were performed by Jaguar from Schrödinger Suite 2018-1,[22] using the local Møller–Plesset second-order (LMP2) method with triple zeta Dunning's correlation consistent basis set[23] and ++ diffuse functions.[24] All calculations were performed in vacuum. The LMP2 method applied to the study of cation–π interactions, showed to be considerably faster than the MP2 method, while the calculated interaction energies and equilibrium distances were almost identical for both methods.[25] Several authors found that LMP2 represents an excellent method for the calculation of interaction energies in proteins.[26,27] Sometimes calculation results can be influenced largely by BSSE (basis set superposition error), and considering it is mandatory, making the calculation times significantly longer. Local correlation methods (such as LMP2) not only reduce the cost of the calculations, but LMP2 is also well known for reducing intramolecular BSSE.[28-30]

The geometries of interacting structures were optimized using LMP2/cc-pVTZ(-f)++ level of theory and their single point energies calculated at LMP2/cc-pVTZ++ level. For the transition metal atoms, we used the LMP2/LACVP** for geometry optimization and LMP2/ /LACV3P** for energy evaluation with effective core potentials (ECPs). The LACV3P basis set is a triple-contraction of the LACVP basis set,[31] developed and tested at Schrödinger, Inc.[22] The optimized geometries were placed in space to match corresponding complexes by superimposing heavy atoms onto their respective coordinates from crystal structures and then the energies of dimeric structures produced in that way were calculated.

The cation–π interaction energies in dimers (cation–π pairs) were calculated as the difference between the energy of the complex and the sum of the energies of the monomers in their optimized geometries.

As mentioned earlier, the energies in this work were calculated in gas phase. When observing *in vitro* processes, we can expect that the water molecules and other atoms and groups from the protein structure could be present in the vicinity, influencing the binding process. To correctly describe the binding, one must be well aware of the role of solvent in the complete process of binding to the proteins. To accurately depict the enthalpy of binding and calculate the interacting energy of bonded structures, high-level quantum mechanical calculations with extended basis sets, including large number of atoms both in protein and ligand as well,

together with water molecules would be needed. But for the complete understanding of biological complexes and their behaviour, the free-energy changes (ΔG) have to be calculated using some statistical mechanics method.[32,33] Recent theoretical studies of the long-range non-covalent interactions in protein side chains showed that the use of the dielectric continuum in order to take the account for the electronic polarization and small backbone fluctuations in proteins a could sometimes lead to decrease in bonding energies for some of those interactions.[32] However, a significant number of cation–π interaction pairs appear to be located in buried regions, thus minimizing the influence on cation–π interactions or direct disruption of the cation–π pairs by water molecules. However, this will exceed the main goal of this article, which is to point out the possible contribution and significance of energies of cation–π interactions to stability and orientation in proteins.

Computation of stabilization centres

Stabilization centres (SC) are defined as the clusters of residues making cooperative, non-covalent long-range interactions.[34] Measured as individual interactions, the stabilization forces resulting from non-covalent long-range interactions are not very strong, but since they are cooperative by their nature, in regions where they act in a group (SC) they could play an important role in maintaining the overall stability of protein structures. In order to analyse SC of interaction-forming residues, we used the SCide program.[35] The criteria SCide uses for determining SC are as follows: 1) two residues are in contact if there is, at least, one heavy atom–atom distance smaller than the sum of their van der Waals radii plus 0.1; 2) a contact is recognized as "long-range" interaction if the interacting residues are, at least, ten amino acids apart; 3) two residues form a stabilization centre if they are in long-range interaction and if it is possible to select one–one residues from both flanking tetrapeptides of these two residues that make, at least, seven contacts between these two triplets.[35]

Computation of conservation of amino acid residues

The conservation of amino acid residues in each protein was computed using the ConSurf server.[36] This server calculates the conservation based on the comparison of the sequence of given PDB chain with the proteins deposited in Swiss–Prot database[37] and identifies ones that are homologous to the PDB sequence. The number of position-specific iteratives (PSI)–BLAST and the *E*-value cut-off used in all similarity searches were 1 and 0.001, respectively. All the sequences, evolutionary related to each one of the proteins in the dataset, were used in the subsequent multiple alignments. Based on these protein sequence alignments, the residues were classified into nine categories, from highly variable to highly conserved. Residues with a score of 1 are considered to be highly variable and residues with a score of 9 are considered to be highly conserved.

RESULTS AND DISCUSSION

The presence of cation−π interactions in key positions in the active site of proteins, provides scope to control the processes, which they regulate and helps in modification or design of new ligand molecules.[38] The quantitative understanding of drug receptor interaction with biological receptors is of prime importance in pharmacy. Therefore, the presence of cation–π interactions could be used as a means of making a difference between chemically relevant docking results and false positives. This scrutiny will assist structural biologist and medicinal chemist to design better and safer drugs.

In this study, we have analysed the influence of cation–π interactions in 43 SOD crystal structures. We have focused our study at the active centres of SOD and hence the cation–π interactions within the rest of the protein structures were not considered. The analysed protein set contains 272 cation–π interactions. We have investigated the structural stability patterns of cation–π interactions in SOD proteins in relation to other environmental preferences like preference of cation–π interaction forming residues, interaction geometries and energetic contribution of cation–π interactions, stabilization centres and conservation patterns.

Preference of cationic and aromatic residues for forming cation–π interactions

The preference of amino acid residues that are involved in cation–π interactions was analysed, and the results are presented in Table I. We observed that in these proteins, among the cationic residues involvement of, Arg in the cation–π interactions is preferred to Lys and His. The number of interactions involving His and Lys residues is almost similar. It is interesting to observe that there is a significant number of Zn^{2+}–π interactions. Among the aromatic residues involved in cation–π interactions, His has the highest occurrence, and the contribution of Phe is twice to that of Trp and Tyr has the lowest occurrence. This might be because His occurs most frequently in both coordination spheres of SOD active centres of all the aromatic amino acids.[9,20] Generally the composition of cation–π interaction forming residues is similar to other globular proteins.[39-42]

TABLE I. Frequency of occurrence of cation–π interaction-forming residues in active centers of superoxide dismutase

Residue	Number[a]	Occurrence[b], %
	Cationic	
Lys^+	20	7.35
Arg^+	197	72.43
His^+	15	5.51
Zn^{2+}	40	14.71
Total	272	100
	Aromatic	
His	135	49.63
Phe	79	29.04
Trp	43	15.82
Tyr	15	5.51
Total	272	100

[a]The number of times a particular amino acid occurs in an appropriate interaction; [b]percent of amino acid occurs in an appropriate interaction

The organization of multicomponent supramolecular assemblies is often governed by multiple non-covalent interactions.[43] Ternary complexes are the simplest model systems where one can understand how pair of cation–π interactions mutually influences each other.[41,44] The specific arrangement or connect-

ivity of cation–π clusters in proteins could significantly influence their structural stability. The analysis shows that around 54 % of the total interacting residues in the dataset are involved in the formation of multiple cation–π interactions. In numerous crystal structures of superoxide dismutases, we found that a cationic residue can interact with several aromatic residues. This type of interaction is marked as furcation. For example, Fig. 3 shows potentially interesting arrangement, the presence of two aromatic groups surrounding one cation. A cation group from A:Arg114 can interact with two aromatic rings of A:Phe49 and A:Phe63 simultaneously. The binding motif between a single cation and two aromatic rings, "π–cation–π", plays a pivotal role in maintaining the acceptor functional structure.[45]

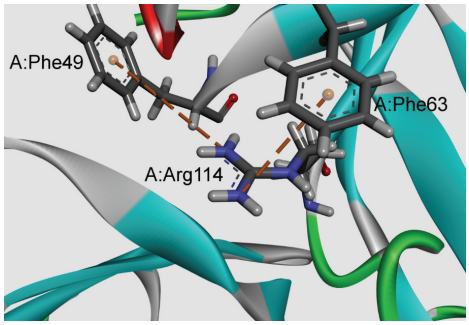

Fig. 3. Example of a multiple cation–π interactions for the cytosolic Cu/Zn SOD from *Schistosoma mansoni* (PDB code 1to4); the interactions are marked with a brown dashed lines.

Interaction geometries and energetic contribution of cation–π interactions

Fig. 4a shows the distribution of distances for cation–π interaction pairs and indicates that these pairs predominantly occur when the residues are separated 0.4 nm or more, without showing a clear geometrical preference. The most favourable distance for the cation–π interacting pairs lies in the range of 0.6–0.7 nm. The distributions of the angle between the cation and the ring plane were in angles (10 to 90° range, with a preference for higher angle values (Fig. 4b), the largest number of pairs occurring between 40 and 80°. These calculations clearly indicate that an effective cation–π interactions can occur across a wider area above the π-ring. The fluctuations are clearly a consequence of their greater flexibility and the geometrical features relating two residue-types are expected to be rather broad.

There are numerous factors that energy of cation–π interaction could depend on: size and electronic structure of the cation, nature of the π-ligand, the directionality and interplay with other noncovalent interactions.[7] The calculated energies of the optimized cation–π interaction pairs range between –451.9 and 20.9 kJ mol^{-1}, with a most populated bin at –4.2 to –29.3 kJ mol^{-1} (Fig. 5). The energies of the most frequent cation–π interactions examined here are in the

lower range of strong hydrogen bonds (–16.8 to –62.8 kJ mol^{-1}), as classified by Desiraju and Steiner.[46]

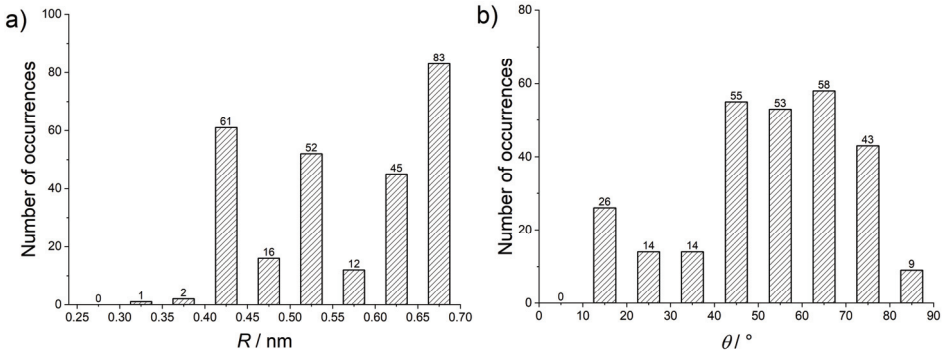

Fig. 4. Interaction geometries of cation–π interactions: a) R distance distribution, b) θ angle distribution.

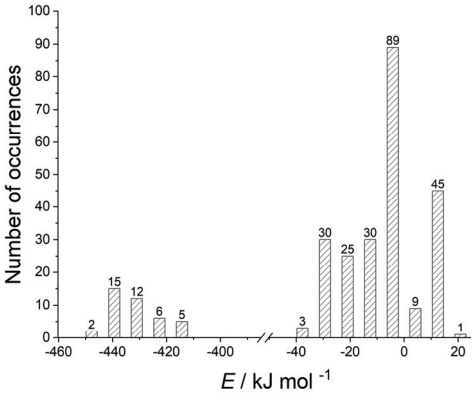

Fig. 5. Interaction energies of cation–π interactions.

The energies calculated for many of the cation–π interactions are substantially stabilizing, with roughly 20 % in this set showing positive (repulsive) predicted interaction energies. The repulsive nature of those interactions emerges from the unfavourable geometries of cation–π interactions in the crystal structures and is usually counterbalanced by other interactions.[20] The strongest attractive interactions (with energies more negative than –418.4 kJ mol^{-1}) arises for the cation–π interactions involving transition metal ions. These interactions, almost strong as covalent ones, owe their strength to the existence of *d* orbitals (strong electrostatic effect caused by the proximity of the metal centre). This range shows that these interactions are among the strongest noncovalent interactions, and most probably plays an important stabilizing role. In Fig. 6, we showed the structural details of the cation–π interaction involving the transition metal ions of bovine Cu/Zn SOD (PDB code 1cbj). Among amino acid the pair

His^+–Trp has strongest attractive interaction (about –29.3 kJ mol^{-1}). The protonated histidine (His^+) is the cation in the cation–π interactions. The cation–π interaction energy of His^+–Trp is larger than other two interaction pairs (His^+–Tyr and His^+–Phe), because of the larger aromatic system in Trp. The indole group of Trp consists of two aromatic rings: one five-membered and one six-membered. Both can take part in cation–π interactions and they can even do this simultaneously. While the cation–π interaction may be weak, they can occur frequently, rendering its overall effect on protein structure significant. Also, when a large network of interactions is considered, cooperativity could emerge, either enhancing or diminishing the overall effect.[43]

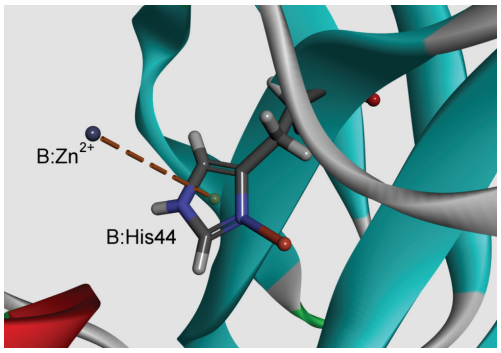

Fig. 6. Example of the cation–π interaction involving transition metal ions of bovine Cu/Zn SOD (PDB code 1cbj). The interaction is marked with a brown dashed line: $B:Zn^{2+}$—B:His44; R = 0.53 nm, θ = 12.42°, E = –436.5 kJ mol^{-1}.

Stabilization centres and conservation of amino acid residues

The performed structural and sequential conservation analysis showed a higher conservation of stabilization centres over protein families.[34] We have computed the stabilization centres for all cation–π interaction forming residues in SOD active centers. Results showed 43 % of cationic residues and 37 % of π-residues having one or more stabilization centres. From the observed results, we infer that all these residues might contribute additional stability to SOD proteins in addition to their participation in cation–π interactions.

An illustrative example of cation–π interaction involving more stabilization centres is showed in Fig. 7. A cation group from A:Arg142 interacts with π-system of A:His62. The three stabilization centres are indicated by wire-meshed surface (red labels). The residue A:Arg142 is part of A51 and A122 stabilization centres while A:His62 is part of A50 stabilization centre.

From our results we assume that most of the residues involved in cation–π interactions are evolutionarily conserved (more than 68 %, with a conservation score ≥ 6) and might have a significant contribution to the stability of SOD proteins.

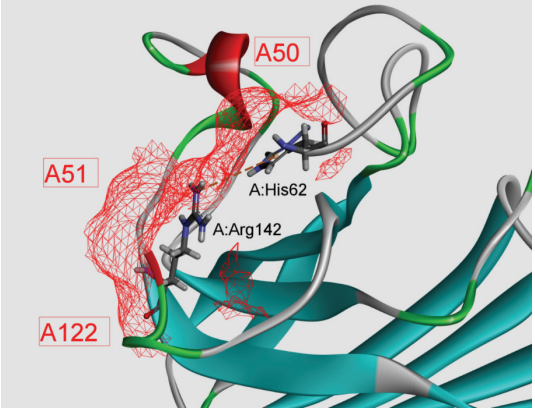

Fig. 7. Details of cation–π interaction involving more stabilization centers at active center of cytosolic Cu/Zn SOD from *Schistosoma mansoni* (PDB ID code 1to4). The cation–π interaction is marked with a brown dashed line (A:Arg142–A:His62; R = 0.676 nm, θ = 72.88°, E = –31.2 kJ mol^{-1}).

CONCLUSION

We have systematically analyzed the influence of cation–π interactions on the stability of SOD active centres. The side chain of Arg is more likely to be in cation–π interactions than Lys and His$^+$ in the cationic residues. His has the highest occurrence in this interaction, more than the other three π-residues, Phe, Tyr and Trp. From the results it can be underlined that around 54 % of the total interacting residues in the dataset are involved in the formation of multiple cation–π interactions. The distribution of distances for cation–π interactions was found to be in the distance range of 0.6–0.7 nm, and the angle distribution with a preference for higher angle values (10 to 90° range). Our results suggest the majority of the cation–π interactions will occur in energy range from −4.2 to −29.3 kJ mol^{-1}. The strongest interactions (with energies more negative than –418.4 kJ mol^{-1}) arise for the cation–π interactions involving transition metal ions. We found that all the residues found in cation–π interactions are important in locating one or more stabilization centres. In the cation–π interacting residues, 68 % of the amino acid residues that are involved in these interactions might be conserved in SOD. From all of that, we could conclude that the contribution of cation–π interactions is an important factor contributing to the structural stability of the SOD active centres that are investigated in this work.

Acknowledgment. The authors would like to thank the Ministry of Education, Science and Technological Development of Republic of Serbia (Grant No: 451-03-68/2022-14/200026 and 451-03-68/2022-14/200168) for financial support.

ИЗВОД

ИСПИТИВАЊЕ УЛОГЕ КАТЈОН–π ИНТЕРАКЦИЈА У АКТИВНИМ ЦЕНТРИМА СУПЕРОКСИД-ДИСМУТАЗА

СРЂАН Ђ. СТОЈАНОВИЋ[1] и МАРИО В. ЗЛАТОВИЋ[2]

[1]Универзитет у Београду – Институт за хемију, технологију и металургију, Београд и [2]Хемијски факултет, Универзитет у Београду, Београд

У овој студији смо анализирали утицај катјон–π интеракција на стабилност и особине активних центара супероксид-дисмутазе (SOD). Број интеракција које формира аргинин је већи од лизина у групи катјона, док је хистидин сразмерно већи у π групи. Енергетски допринос који је резултат најчешћих катјон–π интеракција био је у доњем опсегу јаких водоничних веза. Катјон–π интеракције које укључују јоне прелазних метала као катјон имају енергију негативнију од –418,4 kJ mol^{-1}. Стабилизациони центри ових протеина показали су да су сви остаци укључени у катјон–π интеракције важни у распоређивању једног или више таквих центара. Већина остатака који су укључени у катјон–π интеракције су еволуцијски конзервирани и могли би имати значајан допринос стабилности SOD протеина. Резултати представљени у овом раду могу бити веома корисни за разумевање доприноса катјон–π интеракција стабилности активних центара SOD.

(Примљено 9. јануара, ревидирано 17. фебруара, прихваћено 21. фебруара 2022)

REFERENCES

1. K. A. Dill, *Biochemistry* **29** (1990) 7133 (https://doi.org/10.1021/bi00483a001)
2. J. C. Ma, D. A. Dougherty, *Chem. Rev.* **97** (1997) 1303 (https://doi.org/10.1021/cr9603744)
3. K. S. Kim, P. Tarakeshwar, J. Y. Lee, *Chem. Rev.* **100** (2000) 4145 (https://doi.org/10.1021/cr990051i)
4. R. Wintjens, J. Liévin, M. Rooman, E. Buisine, *J. Mol. Biol.* **302** (2000) 393 (https://doi.org/10.1006/jmbi.2000.4040)
5. J. Cheng, W. Zhu, Y. Tang, Y. Xu, Z. Li, K. Chen, H. Jiang, *Chem. Phys. Lett.* **422** (2006) 455 (https://doi.org/10.1016/j.cplett.2006.03.005)
6. H. Ghiassi, H. Raissi, *J. Sulfur Chem.* **36** (2015) 48 (https://doi.org/10.1080/17415993.2014.962537)
7. N. Kumar, A. S. Gaur, G. N. Sastry, *J. Chem. Sci.* **133** (2021) 97 (https://doi.org/10.1007/s12039-021-01959-6)
8. S. M. Liao, Q. S. Du, J. Z. Meng, Z. W. Pang, R. B. Huang, *Chem. Cent. J.* **7** (2013) 44 (https://doi.org/10.1186/1752-153X-7-44)
9. S. Stojanović, Z. Petrović, M. Zlatović, *J. Serb. Chem. Soc.* **86** (2021) 781 (https://doi.org/10.2298/JSC210321042S)
10. S. Mecozzi, A. P. West, D. A. Dougherty, *J. Am. Chem. Soc.* **118** (1996) 2307 (https://doi.org/10.1021/ja9539608)
11. R. A. Kumpf, D. A. Dougherty, *Science* **261** (1993) 1708 (https://doi.org/10.1126/science.8378771)
12. D. Zhu, B. E. Herbert, M. A. Schlautman, E. R. Carraway, *J. Environ. Qual.* **33** (2004) 276 (https://doi.org/10.2134/jeq2004.2760)
13. L. M. Salonen, M. Ellermann, F. o. Diederich, *Angew. Chem. Int. Ed.* **50** (2011) 4808 (https://doi.org/10.1002/anie.201007560)

14. M. Moradi, A. A. Peyghan, Z. Bagheri, M. Kamfiroozi, *J. Mol. Mod*. **18** (2012) 3535 (https://doi.org/10.1007/s00894-012-1366-7)
15. U. D. Priyakumar, M. Punnagai, G. P. Krishna Mohan, G. N. Sastry, *Tetrahedron* **60** (2004) 3037 (https://doi.org/10.1016/j.tet.2004.01.086)
16. L. Brocchieri, S. Karlin, *Proc. Natl. Acad. Sci. USA* **91** (1994) 9297 https://doi.org/10.1073/pnas.91.20.9297)
17. P. W. Rose, B. Beran, C. Bi, W. F. Bluhm, D. Dimitropoulos, D. S. Goodsell, A. Prlic, M. Quesada, G. B. Quinn, J. D. Westbrook, J. Young, B. Yukich, C. Zardecki, H. M. Berman, P. E. Bourne, *Nucleic Acids Res*. **39** (2011) D392 (https://doi.org/10.1093/nar/gkq1021
18. J. M. Word, S. C. Lovell, J. S. Richardson, D. C. Richardson, *J. Mol. Biol*. **285** (1999) 1735 (https://doi.org/10.1006/jmbi.1998.2401)
19. *Discovery Studio Visualizer, Release 2020*, Accelrys Software Inc., Accelrys Software Inc., San Diego, CA, 2020
20. V. R. Ribić, S. Đ. Stojanović, M. V. Zlatović, *Int. J. Biol. Macromol*. **106** (2018) 559 (https://doi.org/10.1016/j.ijbiomac.2017.08.050)
21. J. Hostaš, D. Jakubec, R. A. Laskowski, R. Gnanasekaran, J. Řezáč, J. Vondrášek, P. Hobza, *J. Chem. Theory Comput.* **11** (2015) 4086 (http://dx.doi.org/10.1021/acs.jctc.5b00398)
22. Schrödinger Release 2018-1: Jaguar, Schrödinger, LLC, New York, 2018
23. T. H. Dunning, *J. Chem. Phys*. **90** (1989) 1007 (https://doi.org/10.1063/1.456153)
24. T. Clark, J. Chandrasekhar, G. n. W. Spitznagel, P. V. R. Schleyer, *J. Comput. Chem.* **4** (1983) 294 (https://doi.org/10.1002/jcc.540040303)
25. A. D. Bochevarov, E. Harder, T. F. Hughes, J. R. Greenwood, D. A. Braden, D. M. Philipp, D. Rinaldo, M. D. Halls, J. Zhang, R. A. Friesner, *Int. J. Quantum Chem*. **113** (2013) 2110 (https://doi.org/10.1002/qua.24481)
26. K. E. Riley, J. A. Platts, J. Řezáč, P. Hobza, J. G. Hill, *J. Phys. Chem., A* **116** (2012) 4159 (https://doi.org/10.1021/jp211997b)
27. G. J. Jones, A. Robertazzi, J. A. Platts, *J. Phys. Chem., B* **117** (2013) 3315 (https://doi.org/10.1021/jp400345s)
28. S. Saebø, W. Tong, P. Pulay, *J. Chem. Phys.* **98** (1993) 2170 (https://doi.org/10.1063/1.464195)
29. A. Reyes, L. Fomina, L. Rumsh, S. Fomine, *Int. J. Quantum Chem.* **104** (2005) 335 (https://doi.org/10.1002/qua.20558)
30. R. M. Balabin, *J. Chem. Phys.* **132** (2010) 231101 (https://doi.org/10.1063/1.3442466)
31. P. J. Hay, W. R. Wadt, *J. Chem. Phys.* **82** (1985) 299 (https://doi.org/10.1063/1.448975)
32. Y. Deng, B. t. Roux, *J. Phys. Chem., B* **113** (2009) 2234 (https://doi.org/10.1021/jp807701h)
33. J. C. Gumbart, B. t. Roux, C. Chipot, *J. Chem. Theory Comput.* **9** (2013) 794 (https://doi.org/10.1021/ct3008099)
34. Z. Dosztányi, A. Fiser, I. Simon, *J. Mol. Biol*. **272** (1997) 597 (https://doi.org/10.1006/jmbi.1997.1242)
35. Z. Dosztányi, C. Magyar, G. Tusnady, I. Simon, *Bioinformatics* **19** (2003) 899 (https://doi.org/10.1093/bioinformatics/btg110)
36. H. Ashkenazy, E. Erez, E. Martz, T. Pupko, N. Ben-Tal, *Nucleic Acids Res.* **38** (2010) W529 (https://doi.org/10.1093/nar/gkq399)

37. B. Boeckmann, A. Bairoch, R. Apweiler, M. C. Blatter, A. Estreicher, E. Gasteiger, M. J. Martin, K. Michoud, C. O'Donovan, I. Phan, S. Pilbout, M. Schneider, *Nucleic Acids Res*. **31** (2003) 365 (https://doi.org/10.1093/nar/gkg095)
38. A. S. Mahadevi, G. N. Sastry, *Chem. Rev.* **113** (2013) 2100 (https://doi.org/10.1021/cr300222d)
39. M. M. Gromiha, *Biophys. Chem*. **103** (2003) 251 (https://doi.org/10.1016/S0301-4622(02)00318-6)
40. B. P. Dimitrijević, S. Z. Borozan, S. Đ. Stojanović, *RSC Adv.* **2** (2012) 12963 (https://doi.org/10.1039/C2RA21937A)
41. S. Z. Borozan, B. P. Dimitrijević, S. Đ. Stojanović, *Comput. Biol. Chem*. **47** (2013) 105 (https://doi.org/10.1016/j.compbiolchem.2013.08.005)
42. I. D. Mucić, M. R. Nikolić, S. Đ. Stojanović, *Protoplasma* **252** (2015) 947 (https://doi.org/10.1007/s00709-014-0727-8)
43. A. S. Mahadevi, G. N. Sastry, *Chem. Rev*. **116** (2016) 2775 (https://doi.org/10.1021/cr500344e)
44. D. Kim, E. C. Lee, K. S. Kim, P. Tarakeshwar, *J. Phys. Chem., A* **111** (2007) 7980 (https://doi.org/10.1021/jp073337x)
45. M. R. Davis, D. A. Dougherty, *Phys. Chem. Chem. Phys*. **17** (2015) 29262 (https://doi.org/10.1039/C5CP04668H)
46. G. R. Desiraju, T. Steiner, *The Weak Hydrogen Bond*, Oxford University Press, Oxford, 1999.